Microscopic observations on microtomed surface of ice

Kinji Hyakutake, Atsushi Moribe, Atsushi Miyamoto,
Kimiko Shimohara and Hitoshi Shoji

Kitami Institute of Technology, 165, Koencho, Kitami 090-8507

Abstract: Surface hollows appearing after microtome shaving were observed on poly- and single crystal specimens under an optical microscope in a cold room laboratory. Characteristic shell-shaped hollows appeared with their major axis perpendicular to the shaving direction. Fewer hollows appeared at specimen surfaces when the basal plane of the ice crystal was parallel or perpendicular to the specimen surface. The results observed could be easily interpreted if cleavage cracks form parallel or perpendicular to the basal plane near the blade edge during the microtome shaving process.

1. Introduction

Microtoming is often applied for surface preparation of ice specimens. However, tiny cracks are generated from the blade edge during the microtoming process, resulting in formation of tiny hollows on the surface. It is important to understand the formation mechanism of these surface hollows for better preparation of sample surfaces, which may be controlled by both 1) the setting conditions of the microtome blade and 2) the ice crystal orientation. This crack/hollow formation may also take place during the cutting process of deep ice cores from polar ice sheets. The c-axis orientation distribution of ice crystals varies with depth in polar ice sheets, which might result in variation of the cutting strength if crystal orientation is a dominant factor.

Experiments were conducted first on polycrystalline ice samples to find out whether there is any difference in appearance of The microtomed surface depending on crystal orientation. Then, single crystal ice samples were taken for detailed examination of anisotropic features by using a lathe. All experiments were conducted in a cold room laboratory at $-20°C$.

2. Experimental method

Polycrystalline ice specimens, which has relatively large grain size and is bubble-free were cut from commercial ice to a size of $3 \times 4 \times 2$ (W $\times$ L $\times$ H) cm. The ice sample frozen onto a glass plate was then mounted on a microtome stage and shaved (Microtome: Leica SM2400). The angle between the upper cutting plane of the blade and the ice surface was set to 30°. The angle between the two cutting planes of the microtome blade was 15° (Fig. 1). The increment of microtome stage height was set to 5 μm for each shaving run. Sliding of the ice sample for microtoming was done manually with a speed of about 25
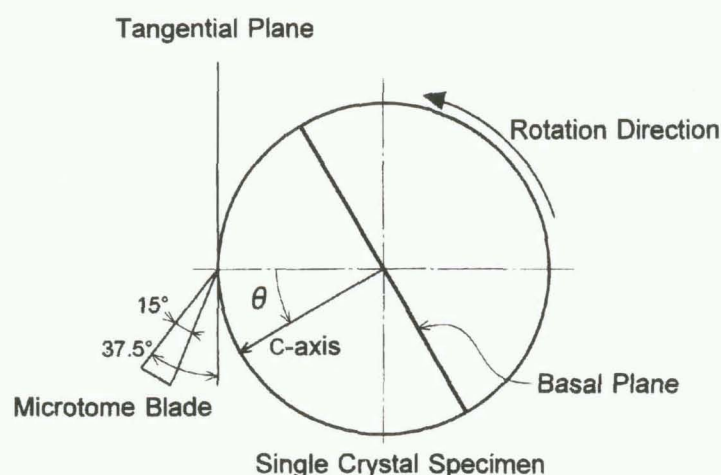
Fig. 1.   *Shaving experiment of a single crystal specimen.*

cm/s, which is almost equivalent to the speed of the cutters of deep drills (Johnsen *et al.*, 1994; Tanaka *et al.*, 1994). The microtomed surface was then examined and photo-recorded under an optical microscope. The microtome blade was exchanged with a new blade after used for 50 times of shaving run.

Single crystal bulk samples approximately 10 cm in diameter and length were produced by using a laboratory-manufactured apparatus (Hyakutake *et al.*, 2000). A $3 \times 3 \times 5$ (W $\times$ H $\times$ L) cm rectangular-shaped piece was cut from the ice sample and lathed to a cylindrical shape 1.8 cm in diameter. Both the c-axis and the a-axis of the specimen were perpendicular to the rotational axis of the cylindrical specimen. Crystal orientations were measured by using the evaporation pit method for both c-axis and a-axis direction determinations (Higuchi, 1958; Matsuda, 1979).

The microtome blade was set to an angle of 37.5° between the upper cutting plane of the blade and the tangential plane of the specimen (Fig. 1). The specimen was rotated at approximately 320 rpm during shaving. The microtomed surface was then examined and photo-recorded under an optical microscope. Photo-recording was completed between 7 and 9 min after shaving. The hollow position at the surface of cylindrical specimen was expressed as the angle θ from the c-axis direction as shown in Fig. 1. Photo-recording was done every 10°, from $\theta = 0°$ to 360°. The recorded area was 357×500 (W $\times$ L) μm. One photo image was taken for each θ for image-analysis using digital image analysis software (NIH image 1.61).

3. Experimental results

A photographic image of a microtomed surface of polycrystalline specimens is shown in Fig. 2. Shell-shaped, surface hollows with a size ranging from a few micrometers to one hundred micrometers were observed under an optical microscope. The extended directions (major axis directions) of the hollows appear almost perpendicular to the shaving direction. Number density and dimensions of the surface hollows can be quite different from one grain to another as shown in Fig. 2 (crystal indicated by dotted line). This result
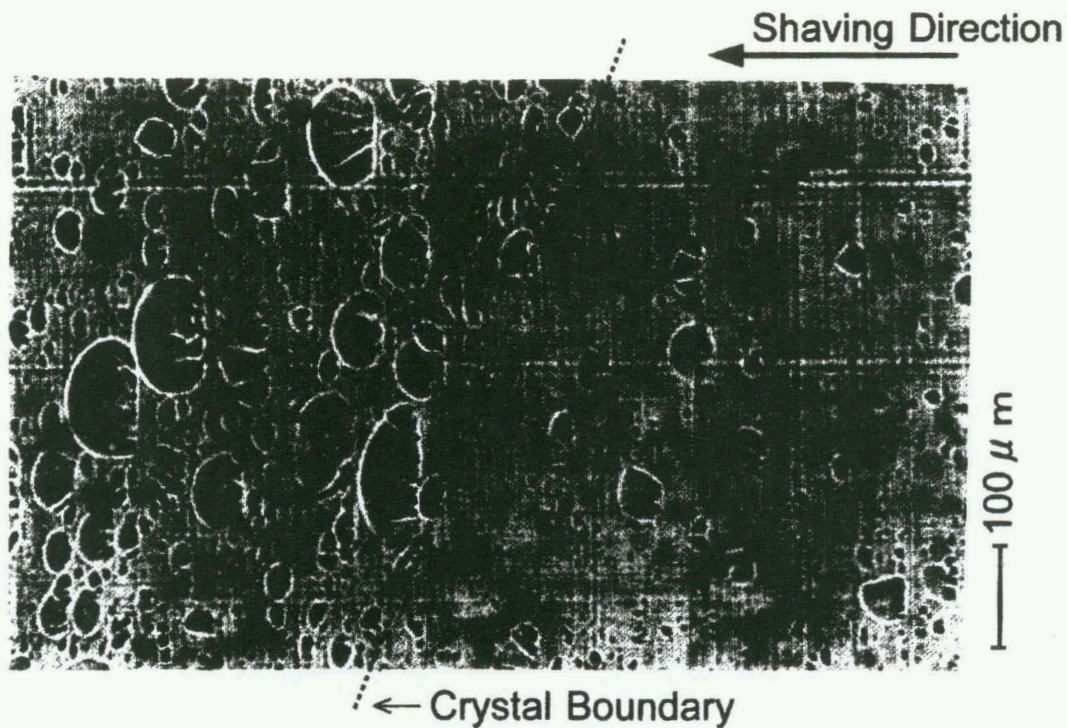
Shaving Direction

← **Crystal Boundary**

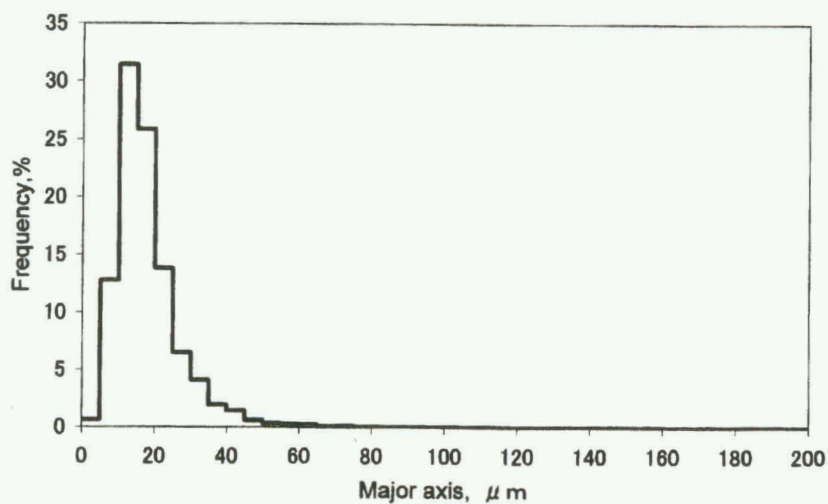*Fig. 2.   Surface hollows after microtome shaving on a polycrystalline specimen.*

Fig. 3.   Size distribution profile of surface hollows on a single crystal specimen.

suggests a strong influence of crystal orientation on size and number density of the surface hollows.

The size distribution of hollows of single crystal specimens was measured and analyzed assuming an ellipsoidal shape for each hollow.   The length of the major axis, A was taken as the size for data treatment.   Most hollows have a major axis smaller than 30
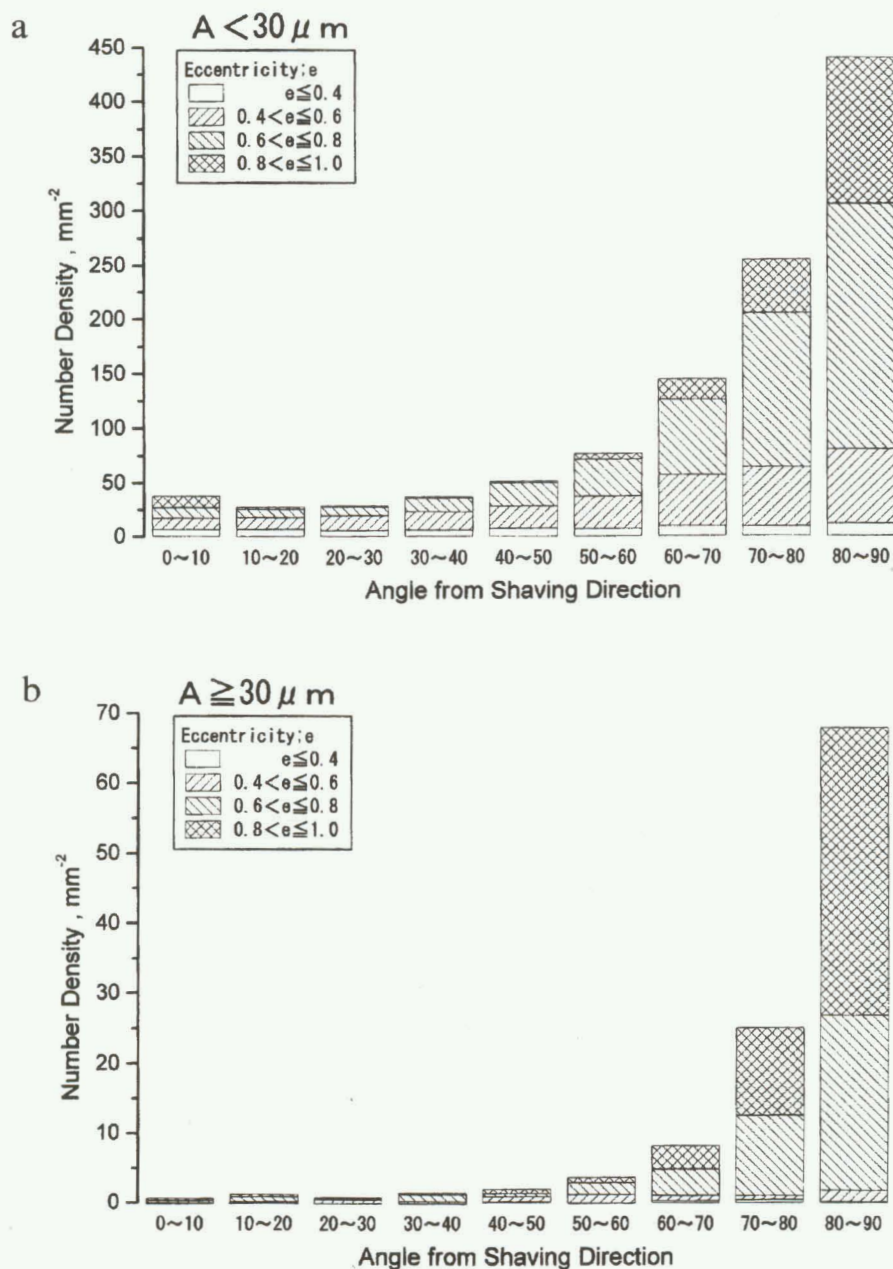
298   K. Hyakutake *et al.*

a

b

Fig. 4.   *Orientation and eccentricity of surface hollow shape: smaller than 30 μm, a; equal to or larger than 30 μm, b (single crystal).*

μm, as shown in Fig. 3.   However, it has been confirmed by another experiment that some very small hollows (smaller than 10 μm size) disappeared due to surface evaporation of the specimen during the few minutes of photo-recording.   Therefore, the appearance frequency of hollows smaller than 10 μm is probably underestimated.   The relation between major axis and minor axis was examined in terms of eccentricity as shown in Fig. 4.   The results clearly show that most hollows have eccentricity values between 0.4 and 1, with their major
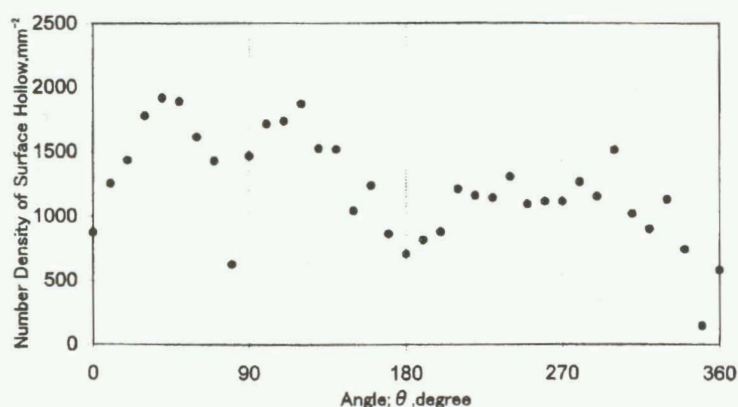
Fig. 5. A number density profile of surface hollows on a single crystal specimen.
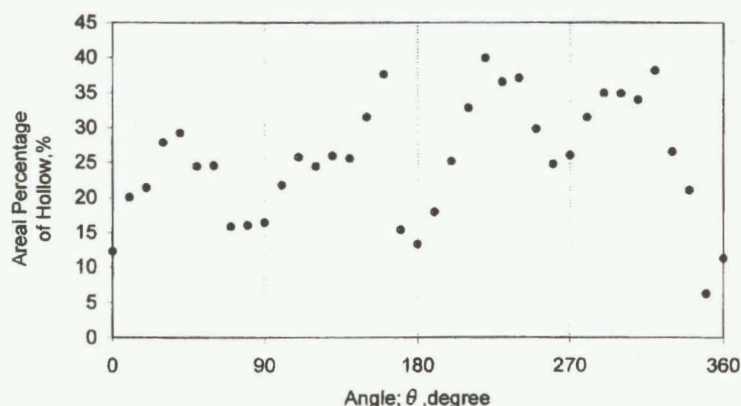

Fig. 6. Areal percentage occupied by surface hollows.

axis direction perpendicular to the shaving direction. This trend is much clearer for those larger than 30 μm, as shown in Fig. 4b.

In Fig. 5 the number density, N, of surface hollows of the single crystal specimen is plotted against the angle θ. When $\theta=0$, the basal plane is parallel to the tangential plane at the tip of the microtome blade. A relation was observed between N and θ, with lower values of N around θ values of 0, 90, 180, 270 and 360°. Conditions for θ and $\theta+180°$ are equivalent. Therefore, N values at $\theta=0$ and 90° should be compared with N values at $\theta=180/360$ and 270° respectively.

The total area of hollows projected to a plane parallel to the specimen surface (tangential plane), S, was measured and analyzed per unit area of the specimen surface. S, plotted against θ (Fig. 6), also shows lower values around θ close to 0, 90, 180, 270 and 360°.

Both N and S values should be affected by surface evaporation during the photo-recording period, but the appearance of negative peaks is well preserved in both the $0 < \theta < 180$ region and the $180 < \theta < 360$ region. N $(0 < \theta < 180)$ is generally larger than N $(180 < \theta < 360)$, which might result from the surface evaporation. Because photo-recording proceeded from $\theta=0$ toward increasing θ, hollows in an area of larger θ values had more

300   K. Hyakutake *et al.*

time for sublimation. S $(0 < \theta < 180)$ is, however, smaller than S $(180 < \theta < 360)$, which suggests that the differences in N and S could be caused by other unknown factors in addition to the sublimation effect.

4. Discussion

These findings show that a smoother surface can be obtained under a shaving condition of θ close to 0 or 90° relative to the c-axis in case of single crystal.   Tiny cracks are generated from the blade edge during the microtoming process.   When most cracks propagate parallel to the specimen surface, there should be few hollows generated at the surface during shaving.   This could be the case for the $\theta = 0°$ condition where cracks generated might be of cleavage crack origin along the basal plane of the ice crystal.   This condition could also be the case for $\theta = 90°$ if a plane perpendicular to the a-axis can be activated to cause cleavage.

The experimental results obtained suggest that in ice drilling near a depth in polar ice sheets at which most c-axes are parallel to the vertical direction, fewer cracks will penetrate downward compared to ice drilling of random orientation fabrics.   Such penetration might cause difficulty in drill penetration if other factors stay constant.

C-axes of ice crystals become preferentially oriented in the vertical direction of the Dye 3, Greenland deep ice core with depth (Herron *et al.*, 1985).   The specific cutting energy, the energy to produce 1 m^3 of cuttings, increased with depth in spite of improvements in the cutting system at Dye 3, Greenland (Gundestrup and Johnsen, 1985).   This increase in the specific energy might be caused by the change in the crack formation characteristics.

Acknowledgments

References

Gundestrup, N.S. and Johnsen, S.J. (1985): A battery powered, instrumented deep ice core drill for liquid filled holes.   Greenland Ice Core: Geophysics, Geochemistry, and the Environment, ed. by C.C. Langway, Jr. *et al*. Washington, D.C., Am. Geophys. Union, 19–22 (Geophysical Monograph 33).

Herron, S.L., Langway, C.C., Jr. and Brugger, K.A. (1985): Ultrasonic velocities and crystalline anisotropy in the ice core from Dye 3, Greenland.   Greenland Ice Core: Geophysics, Geochemistry, and the Environment, ed. by C.C. Langway, Jr. *et al*. Washington, D.C., Am. Geophys. Union, 23–31 (Geophysical Monograph 33).

Higuchi, K. (1958): The etching of ice crystals.   Acta Metall., **6**, 636–642.

Hyakutake, K., Fukuda, A. and Shoji, H. (2000): Growth of ice single crystal.   Mem. Kitami Inst. Tech., **32**, 27–36 (in Japanese with English abstract).

Johnsen, S.J., Gundestrup, N.S., Hansen, S.B., Schwander, J. and Rufli, H. (1994): The new improved version of the ISTUK ice core drill. Mem. Natl Inst. Polar Res., Spec., Issue, **49**, 9–23.

Matsuda, M. (1979): Determination of a-axis orientations of polycrystalline ice. J. Glaciol., **22**, 165–169.

Tanaka, Y., Takahashi, A., Fujii, Y., Narita, H., Shinbori, K., Azuma, N. and Watanabe, O. (1994): Development of a JARE deep ice core drill system. Mem. Natl Inst. Polar Res., Spec., Issue, **49**, 113–123.